J. Fluid Mech. (1978), *vol.* 85, *part* 2, *pp.* 349–368
Printed in Great Britain

Vapour-bubble growth in a superheated liquid

By ANDREA PROSPERETTI
Istituto di Fisica, Università degli Studi, Milan, Italy
AND MILTON S. PLESSET
Engineering Science Department, California Institute of Technology, Pasadena

(Received 19 January 1977)

It is shown that the approximation of a thin thermal boundary layer gives an accurate description of the growth of spherical vapour bubbles in a superheated liquid except for very small superheats. If the further approximations of a linear variation of vapour pressure with temperature and of constant physical properties are made, then scaled variables can be introduced which describe the growth under any conditions. This scaled description is not valid during the early, surface-tension dominated, portion of the growth. The rate of bubble growth for large superheats is somewhat overestimated in the intermediate stage in which both inertial and thermal effects play a role. This overestimate does not lead to a serious error in the radius–time behaviour for ranges of practical interest. The asymptotic, or thermally controlled, stage of growth is accurately described by the scaled formulation.

1. Introduction

The theory of the growth of a vapour bubble in a superheated liquid has been considered by several authors (Plesset & Zwick 1954, 1955; Birkhoff, Margulies & Horning 1958; Scriven 1959; Zwick 1960; Bankoff 1964; Theofanous *et al.* 1969; Mikic, Rohsenow & Griffith 1970; Dalle Donne & Ferranti 1975; Theofanous & Patel 1976) in part at least because of theoretical implications for boiling heat transfer (see, for example, Rohsenow 1971) and for other problems in two-phase flows. Even with the simplifying assumption of spherical symmetry the formulation and solution of the problem are somewhat complex, and attempts have been made to obtain some analytical expressions of relatively simple form. These approximations, however, are either limited in their range of applicability to the late stages of bubble growth (Plesset & Zwick 1954; Birkhoff *et al.* 1958; Scriven 1959) or do not have a stronger theoretical foundation than that of being *ad hoc* interpolations between the correct limiting solutions for large and small times (Mikic *et al.* 1970).

The primary objective of the present study is to present a law of bubble growth which has a clear physical basis and which, although somewhat simplified, retains a large degree of accuracy and applicability in the range of bubble radii of practical interest. While it has not been possible to obtain a general solution in closed analytical form, it will be shown that, with appropriate scaling, bubble growth can be described under general conditions of liquid superheat and liquid properties by a single equation that does not contain any parameter. This 'universal' law of growth is valid only for bubbles that have grown by about an order of magnitude beyond their initial radius,

so that surface-tension effects have become unimportant. This limitation is inconsequential in practice, particularly for moderate and large liquid superheats.

Our approach is based on the theory developed by Plesset & Zwick (1954), who gave an approximate solution to the energy equation (Plesset & Zwick 1952). A secondary objective of the present study is to show that this theory gives quite good results unless the liquid superheat is very small. Its accuracy is demonstrated by the close agreement with the results of Dalle Donne & Ferranti (1975), who solved by detailed numerical integration the complete set of partial and ordinary differential equations for the growth problem. The approximate formulation that leads to the description in terms of scaled variables is also shown to be in agreement with the results of Dalle Donne & Ferranti (1975) in the range of bubble radii of concern in practice.

The interpolation expression obtained by Mikic *et al.* (1970) is also considered here. With the modification suggested by Theofanous & Patel (1976), the scaled variables of Mikic *et al.* coincide with ours, and their interpolation scheme is found to give acceptable results.

2. The analytical model

The nucleus from which the vapour bubble will eventually grow is supposed to be a spherical cavity of radius R_0 in a liquid at the uniform temperature T_∞. The internal pressure in the nucleus will be taken to be the equilibrium vapour pressure $p_v(T_\infty)$, for the liquid temperature, and the equilibrium radius is then

$$R_0 = 2\sigma/[p_v(T_\infty) - p_\infty], \tag{1}$$

where σ is the surface tension at the temperature T_∞ and p_∞ denotes the ambient liquid pressure, which is supposed to be constant. The pressure p_∞ corresponds to a well-defined equilibrium temperature, the 'boiling' temperature T_b. Equation (1) implies that $T_\infty > T_b$, and the difference $\Delta T = T_\infty - T_b$ is termed the liquid superheat. This simple model for the vapour nucleus is certainly idealized, but it may be shown that initial conditions do not have a significant effect on the subsequent growth of a bubble (see, for example, figure 11 below).

The equilibrium described by (1) is unstable, and a perturbation can result in the growth of the nucleus. In the initial, or latent, stage the radial velocity of growth is limited by the restraining effect of surface tension, which becomes of decreasing importance with increasing bubble radius. If the initial superheat is sufficiently large, the limiting factor in the following stage of growth will be the liquid inertia. An upper bound for the growth velocity will then be given by

$$\left(\frac{dR}{dt}\right)_{\text{inertial}} = \left[\frac{2}{3}\frac{p_v(T_\infty) - p_\infty}{\rho}\right]^{\frac{1}{2}}, \tag{2}$$

where R is the bubble radius and ρ is the liquid density. The increase in bubble volume requires a corresponding inflow of thermal energy in order that the volume remains filled with vapour. The rate of inflow of energy to meet the latent-heat requirement is clearly proportional to $R^2 dR/dt$, so that the inertial growth stage will be followed by an intermediate stage in which both inertial and thermal effects control the growth. Finally, in the asymptotic stage for large radius, the only important controlling factor

will be the inflow of thermal energy. In this stage, the familiar expression for the growth velocity applies:

$$\left(\frac{dR}{dt}\right)_{\text{thermal}} = \left(\frac{3}{\pi}\right)^{\frac{1}{2}} \frac{k}{L\rho_v(T_b)} \frac{T_\infty - T_b}{(Dt)^{\frac{1}{2}}}, \tag{3}$$

in which k is the liquid thermal conductivity, L is the latent heat, $\rho_v(T_b)$ is the equilibrium vapour density at the boiling temperature, and D is the thermal diffusivity of the liquid. This equation expresses the balance between the rate of heat flow in the liquid to the bubble wall, given approximately by $4\pi R^2 k\Delta T/(Dt)^{\frac{1}{2}}$, and the latent heat required to supply the vapour in the bubble at the temperature T_b, which is of the order of $4\pi R^2 L\rho_v(dR/dt)$ (Plesset & Zwick 1954; Plesset & Prosperetti 1977).

The detailed results which follow will show that the growth stages just described apply only for sufficiently large liquid superheats. For smaller superheats, the inertial stage may never be reached, the latent stage passing directly into the intermediate stage; at still smaller superheats, the latent stage will be followed directly by the asymptotic stage. At the other extreme of very large initial superheats, the intermediate or the asymptotic stage would be reached only for bubble radii so large as to be of no practical significance. This behaviour is, for example, characteristic of cavitation bubbles.

We may note that integration of (3) gives

$$R \sim 2k\left(\frac{3}{\pi D}\right)^{\frac{1}{2}} \frac{(T_\infty - T_b)}{L\rho_v(T_b)} t^{\frac{1}{2}}, \tag{4}$$

which is a frequently used result. It must be emphasized that it is valid only for times large enough for the growth velocity to be much smaller than the inertia-controlled velocity. This behaviour will be discussed further below.

With the assumption of spherical symmetry, the continuity and momentum equations for an incompressible liquid give the Rayleigh equation (see, for example, Plesset & Prosperetti 1977)

$$R\frac{d^2R}{dt^2} + \frac{3}{2}\left(\frac{dR}{dt}\right)^2 = \frac{1}{\rho}\left\{p_v(T_s) - p_\infty - \frac{2\sigma}{R}\right\}. \tag{5}$$

The liquid temperature at the bubble surface is $T_s(t)$, and it is assumed that the vapour in the bubble has uniform density and pressure and is in thermodynamic equilibrium at the temperature T_s. Non-equilibrium effects can be shown to be small if the accommodation coefficient is not appreciably less than unity. An additional assumption contained in (5) is that viscous effects may be neglected. Viscous effects could be accounted for by including the term $-4(\nu/R)(dR/dt)$ in the right-hand side of (5). For the liquids of present concern, such as water or liquid sodium, the kinematic viscosity ν is so small that viscous effects are negligible.

The liquid temperature T_s at the bubble boundary must be obtained from the solution of the energy equation, which here takes the form

$$\frac{\partial T}{\partial t} + \frac{R^2}{r^2}\frac{dR}{dt}\frac{\partial T}{\partial r} = \frac{D}{r^2}\frac{\partial}{\partial r}\left(r^2\frac{\partial T}{\partial r}\right), \tag{6}$$

where r is the radial distance measured from the centre of the bubble and $T = T(r, t)$. Clearly

$$T_s(t) = T(R(t), t). \tag{7}$$

We should note that the form of the energy equation in (6) implies the neglect of the temperature dependence of the thermal conductivity of the liquid but not of the temperature dependence of its density or of its specific heat.

At the moving boundary $r = R(t)$, the temperature field is subject to the condition

$$4\pi R^2 k \left(\frac{\partial T}{\partial r}\right)_{r=R(t)} = L\frac{d}{dt}[\tfrac{4}{3}\pi R^3 \rho_v(T_s)], \tag{8}$$

which expresses the requirement that the energy conducted from the liquid into the bubble equals the product of the latent heat L and the rate of vapour production. Further conditions on the temperature field are

$$T(r,0) = T_\infty, \tag{9a}$$

$$T(r,t) \to T_\infty \quad \text{as} \quad r \to \infty. \tag{9b}$$

3. The thermal problem

A solution of the heat-flow equation (6) with conditions (9) and with arbitrary time-varying heat flux at the bubble surface may be obtained subject to suitable approximations. This result, which was obtained by Plesset & Zwick (1952), greatly simplifies the solution of the growth problem. This solution is summarized here with the dual purpose of completeness of the present discussion and of clarifying the range of validity of the approximations introduced. There has been some confusion in the literature regarding the latter point.

The heat-flow equation (6) is complicated by the presence of the convective term on the left-hand side. This term can be formally eliminated by introduction of a Lagrangian independent variable

$$h = \tfrac{1}{3}(r^3 - R^3), \tag{10}$$

in terms of which (6) becomes

$$D\frac{\partial}{\partial h}\left(r^4 \frac{\partial T}{\partial h}\right) = \frac{\partial T}{\partial t}. \tag{11}$$

It is also convenient to introduce a transformed time variable u defined as

$$u = \int_0^t R^4(t')\,dt', \tag{12a}$$

and a new dependent variable U given by

$$U(h,t) = \int_r^\infty r'^2[T_\infty - T(r',t)]\,dr' = \int_h^\infty [T_\infty - T(h',t)]\,dh'. \tag{12b}$$

For constant liquid density and specific heat, U is proportional to the thermal energy removed from the liquid exterior to the sphere of radius r by the latent-heat requirement of the vapour bubble. If (11) is integrated from h to infinity, one obtains for constant D

$$D(1 + 3h/R^3)^{\frac{4}{3}} \frac{\partial^2 U}{\partial h^2} = \frac{\partial U}{\partial u}, \tag{13}$$

and conditions (9) become

$$U(h,0) = 0, \tag{14a}$$

$$U(h,u) \to 0 \quad \text{as} \quad h \to \infty. \tag{14b}$$

Let us now suppose that the temperature gradient is appreciable only in a thermal boundary layer about the bubble of thickness $\delta \simeq (Dt)^{\frac{1}{2}}$. Then, with neglect of terms of second and higher order in δ/R, one may write

$$\frac{h}{R^3} = \frac{r-R}{R}\frac{r^2+rR+R^2}{3R^2} \lesssim \frac{\delta}{R}.$$

An estimate of the magnitude of δ/R may be obtained by use of (4), and with the neglect of unimportant numerical factors one finds

$$\frac{\delta}{R} \sim \frac{DL\rho_v}{k(T_\infty - T_b)} = \frac{\rho_v}{\rho}\frac{L}{c(T_\infty - T_b)}, \tag{15}$$

where c is the specific heat of the liquid. The reciprocal of the right-hand side of (15) is often referred to as the Jakob number (Zuber 1961) and it should be noted that it is independent of the thermal conductivity k of the liquid. By way of example, for water at 100 °C one has $\delta/R \simeq 0{\cdot}38/\Delta T$ and for sodium at 890 °C one has $\delta/R \simeq 2{\cdot}9/\Delta T$. It is evident that even for modest superheats one may make the approximation that $h/R^3 \ll 1$. Equation (13) then becomes to lowest order

$$D\,\partial^2 U/\partial h^2 = \partial U/\partial u, \tag{16}$$

which is the standard form of the diffusion equation. The general solution of (16) which satisfies the conditions (14) and which has $\partial^2 U/\partial h^2$ given at $h = 0$ as an arbitrary function of time is readily found by Laplace transform methods (see Plesset & Zwick 1952). When the solution is written in the original variables, we have

$$T_s(t) = T_\infty - \left(\frac{D}{\pi}\right)^{\frac{1}{2}} \int_0^t \frac{R^2(x)}{\left[\int_x^t R^4(y)\,dy\right]^{\frac{1}{2}}} \frac{\partial T(R(x),x)}{\partial r}\,dx, \tag{17}$$

where $\partial T(R(t),t)/\partial r$ is the arbitrarily prescribed gradient at the bubble wall. We may note that for constant R this expression reduces to the well-known result for a plane interface

$$T_s(t) = T_\infty - \left(\frac{D}{\pi}\right)^{\frac{1}{2}} \int_0^t (t-x)^{-\frac{1}{2}} \frac{\partial T(R,x)}{\partial r}\,dx. \tag{18}$$

For the bubble growth problem, the boundary condition (8) should be used in (17) to give

$$T_s(t) = T_\infty - \frac{1}{3k}\left(\frac{D}{\pi}\right)^{\frac{1}{2}} \int_0^t L\frac{d}{dx}[R^3\rho_v(T_s)]\left[\int_x^t R^4(y)\,dy\right]^{-\frac{1}{2}} dx. \tag{19}$$

To be consistent with the assumptions already made, k and D should be taken to be independent of temperature, but no such assumption has been made thus far for L and ρ_v. In order to ensure a correct description of the asymptotic stage, k and D should be evaluated at the boiling temperature T_b.

The method followed to deduce (17) is essentially that of matched asymptotic expansions with (16) representing the lowest-order inner equation and the corresponding outer solution to lowest order being $U(h,t) = 0$. Plesset & Zwick (1952) have also considered first-order terms and give an explicit expression for the correction to (17).

A further remark may be made concerning the estimate of the quantity δ/R. As already pointed out, at sufficiently high liquid superheats, the initial growth has

approximately the constant inertial velocity given by (2). The rate of change of the thermal boundary layer for early times has large values which are proportional to $t^{-\frac{1}{2}}$. It is therefore pertinent to inquire whether $\delta \ll R$ at the initiation of the intermediate stage when thermal effects begin to be important. This stage begins approximately at the time t_0 at which the inertial growth velocity (2) and the thermal growth velocity (3) are roughly equal. We have therefore

$$\frac{\delta(t_0)}{R(t_0)} \simeq \frac{(Dt_0)^{\frac{1}{2}}}{R_0 + (dR/dt)_{\text{inertial}}\, t_0} < \left(\frac{D}{t_0}\right)^{\frac{1}{2}} \left(\frac{dR}{dt}\right)^{-1}_{\text{inertial}}$$

and, since at t_0 we have $(dR/dt)_{\text{inertial}} = (dR/dt)_{\text{thermal}}$,

$$\frac{\delta(t_0)}{R(t_0)} \lesssim \frac{\rho_v}{\rho_l} \frac{L}{c(T_\infty - T_b)},$$

which agrees with our previous estimate (15).

4. The growth analysis

The dynamical equation (5) and the solution to the energy equation (19) are coupled by the thermodynamic equilibrium relation $p_v = p_v(T_s)$, so that the solution to the growth problem is determined subject to the simplifications which have been introduced. A way of assessing the consequences of these approximations is to compare the results obtained in this way with results derived on the basis of a more accurate model. Such a study has recently been performed by Dalle Donne & Ferranti (1975), who solved the system of equations (5) and (6) numerically without introducing the hypothesis of a thin thermal boundary layer; these authors used the equilibrium pressure–temperature relationship.† The numerical results of Dalle Donne & Ferranti are compared with the results of the approximations in figures 1–3 for a range of ambient pressures and superheats. In these figures the continuous lines show the results obtained from (5) and (19)‡ and the open circles show Dalle Donne & Ferranti's values; the broken lines will be discussed below. The numbers labelling the curves refer to table 1, which gives the physical conditions for the various examples. The most stringent comparisons are those between the growth velocities (figure 1) and the surface temperatures (figure 2), rather than that between the radii (figure 3). Figure 1(*a*) shows the growth velocities of bubbles at an ambient pressure of $p_\infty = 1$ atm ($T_b = 1155$ °K) for liquid-sodium superheats of 279, 133 and 22 °K. The comparison is quite good except in the early stages of growth, where the slightly different initial conditions used in the present work result in some discrepancies which, however, have no consequences for the later behaviour. Figure 3(*a*) confirms this observation.

† It should be pointed out that equation (24) of the paper by Dalle Donne & Ferranti (1975), which corresponds to our equation (8), is incorrect in that the latent heat is within the time-derivative operator, and further because the expansion work and surface energy are improperly introduced (see, for example, Hsieh 1965). In addition, instead of separating the liquid thermal conductivity and the ρc factor in the energy equation, they use the same form as our equation (6), with the thermal diffusivity taken to be a function of the local temperature. While the alteration of the boundary condition (8) is certainly of negligible importance in view of the smallness of the terms improperly introduced, the error in the energy equation may be somewhat more significant, although it is not expected to alter their results substantially.

‡ Details of the numerical method used to obtain the results will be made available elsewhere.

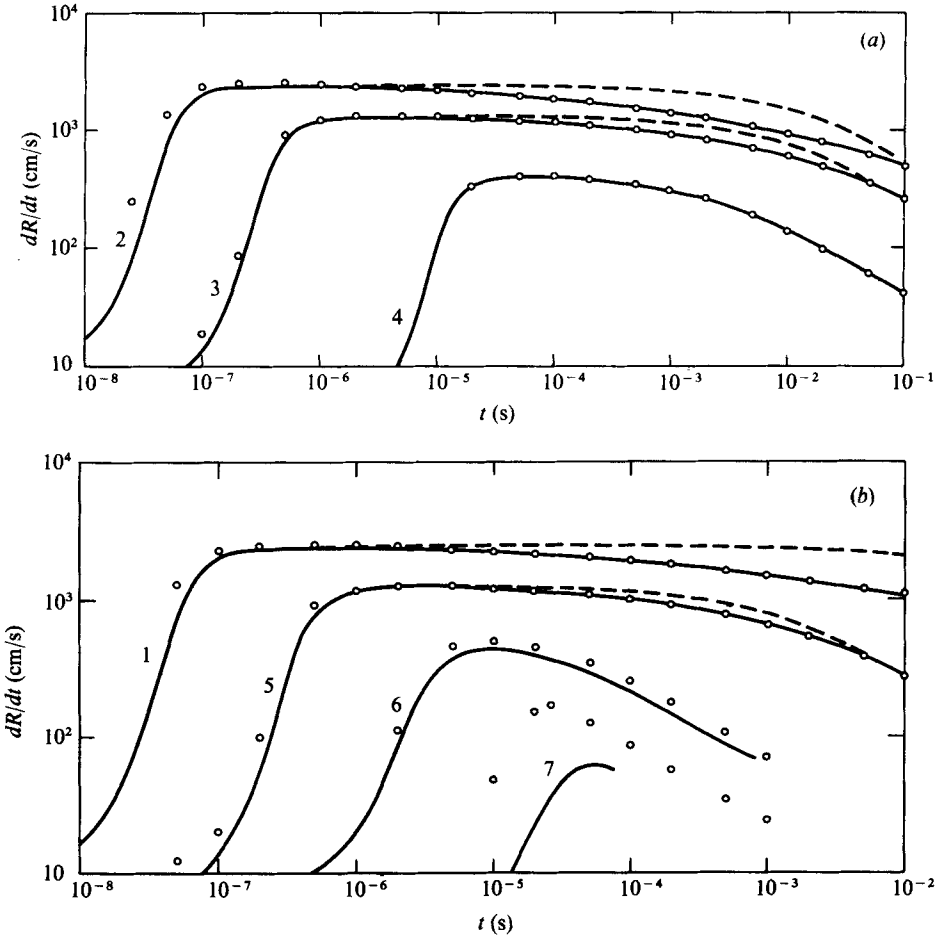

FIGURE 1. Growth rates of vapour bubbles in superheated sodium. The continuous lines have been obtained from (5) and (19) and the dashed lines from (24). Only the continuous line is shown where the two coincide. The numbers labelling the curves refer to table 1, which gives the physical conditions for the examples shown. The open circles are the results of Dalle Donne & Ferranti (1975).

Figure 1(*b*) represents the results for a case of very high superheat ($p_\infty = 0{\cdot}5$ atm, $\Delta T = 340\,^\circ$K), a case of moderate superheat ($p_\infty = 2$ atm, $\Delta T = 90\,^\circ$K) and two cases of small superheat ($p_\infty = 4{\cdot}5$ atm, $\Delta T = 15\,^\circ$K and $p_\infty = 6$ atm, $\Delta T = 5\,^\circ$K). While the cases of high and moderate superheat follow the behaviour encountered in the previous cases, the examples with low superheat, and especially the second one, show a poorer agreement: the assumption of small δ/R (large Jakob number) is not valid for these bubbles and other terms in the solution of (13) become important. Much the same trend is observed in the surface temperature behaviour (figure 2). It should be remarked that the rapid increase in the value of δ/R (see table 1) is brought about more by the increase in ρ_v with temperature than by the decrease in ΔT. Finally we remark that the data of Dalle Donne & Ferranti indicated in figures 1–3 have been obtained from copies of their original figures: this circumstance explains the occasional scatter in their points which appears in our figures.

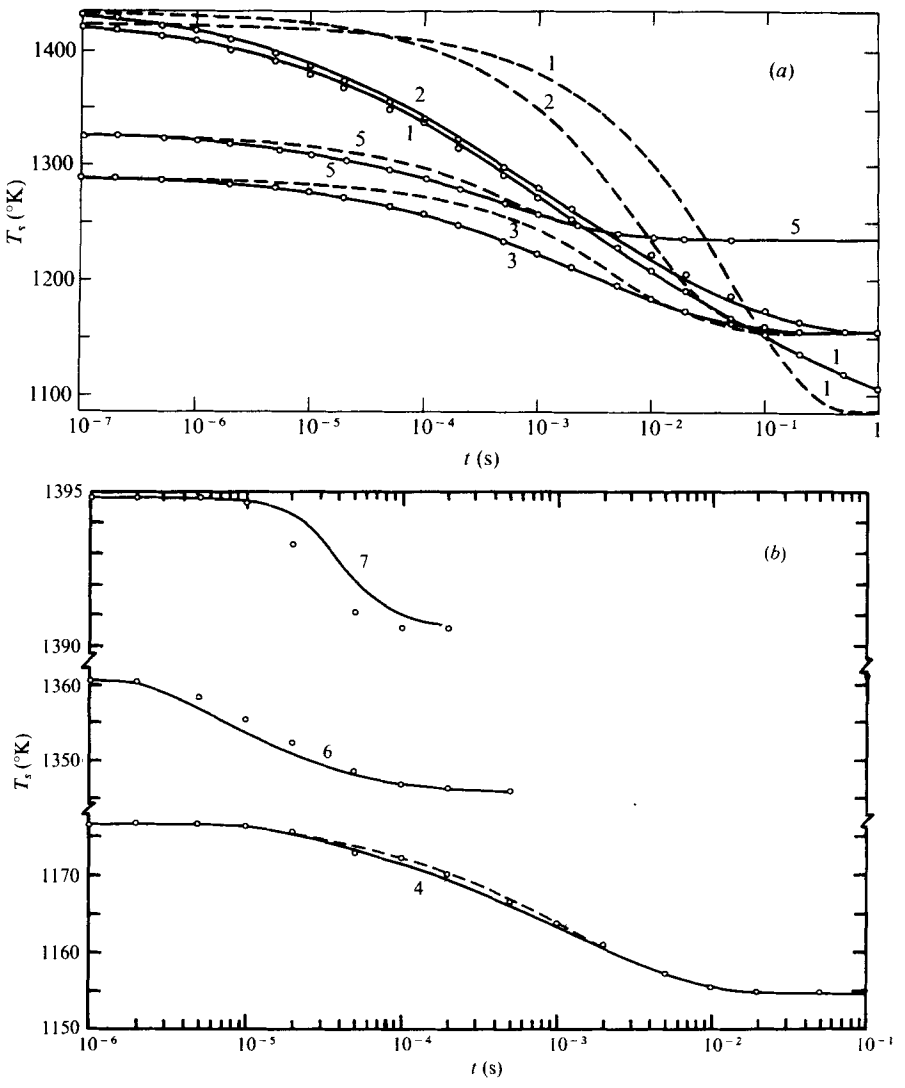

FIGURE 2. Bubble surface temperatures during growth in superheated sodium. The continuous lines have been obtained from (5) and (19) and the dashed lines from (24). The numbers labelling the curves refer to table 1, which gives the physical conditions for the examples shown. The open circles are the results of Dalle Donne & Ferranti (1975).

We now proceed to obtain an approximate scaling law for bubble growth of general applicability. To this end we make some approximations as follows. First we shall take L and ρ_v to be independent of temperature and we shall evaluate them at the boiling temperature T_b. This choice, rather than T_∞, say, will ensure that the last stage of bubble growth, the thermally controlled stage, will be more correctly described. Second, we shall approximate the relation between the equilibrium vapour pressure and the temperature by a linear relation (see figure 4):

$$p_v(T_s) = p_v(T_\infty) - \frac{p_v(T_\infty) - p_\infty}{T_\infty - T_b}(T_\infty - T_s). \tag{20}$$

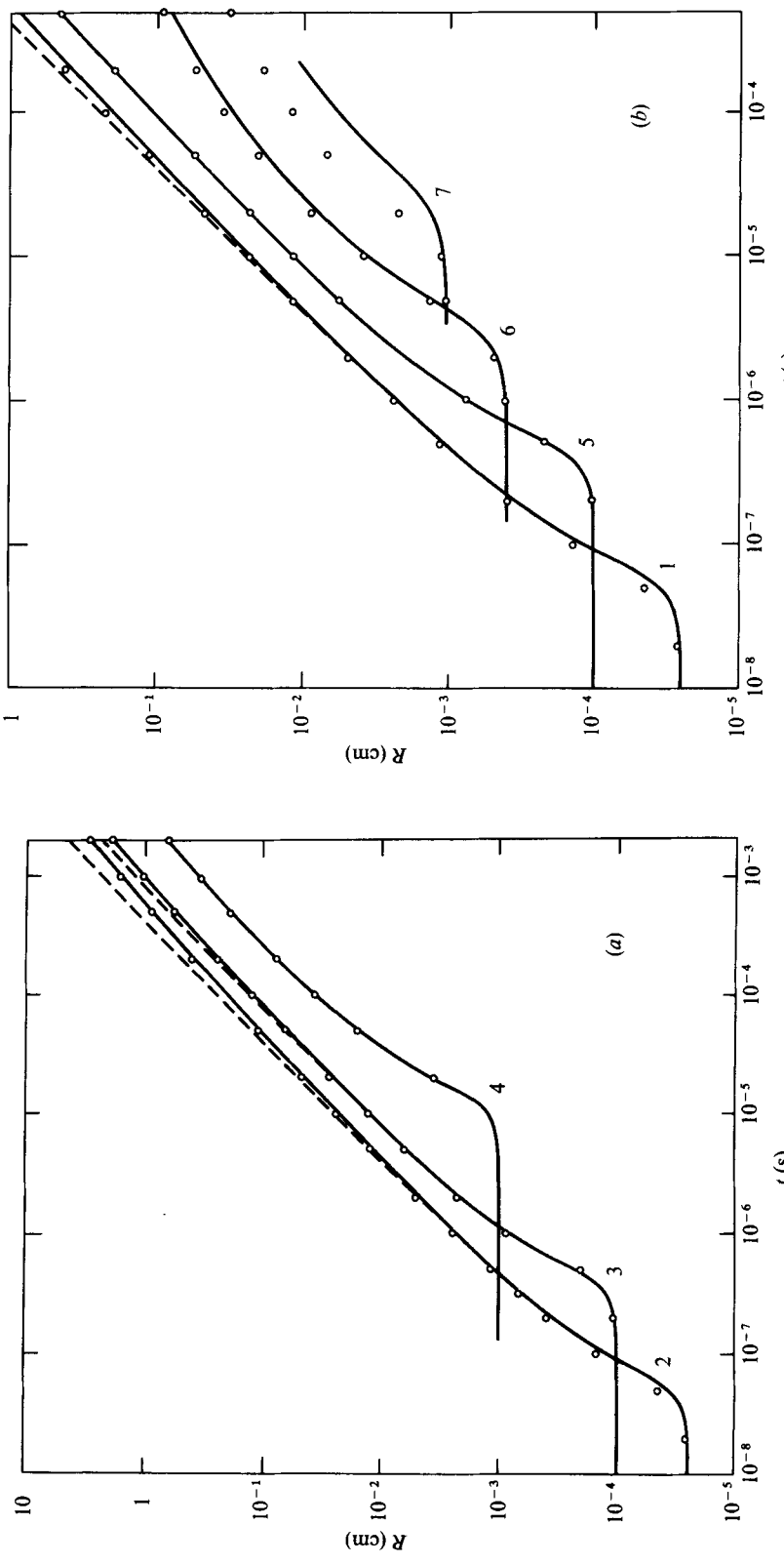

FIGURE 3. Radius *vs.* time for vapour bubbles growing in superheated sodium. The continuous lines have been obtained from (5) and (19) and the dashed lines from (24). Only the continuous line is shown where the two coincide. The numbers labelling the curves refer to table 1, which gives the physical conditions for the examples shown. The open circles are the results of Dalle Donne & Ferranti (1975).

Bubble	T_b (°K)	ΔT (°K)	p_∞ (atm)	R_0 (cm)	μ	α	δ/R (eq. 15)	Jakob no.
1	1083·6	340·1	0·5	$2{\cdot}5\times10^{-5}$	$1{\cdot}253\times10^{-4}$	$1{\cdot}647\times10^{7}$	$1{\cdot}77\times10^{-3}$	565·7
2	1154·6	278·9	1	$2{\cdot}5\times10^{-5}$	$3{\cdot}212\times10^{-4}$	$1{\cdot}224\times10^{8}$	$4{\cdot}39\times10^{-3}$	227·7
3	1154·6	133·1	1	10^{-4}	$9{\cdot}899\times10^{-4}$	$1{\cdot}655\times10^{7}$	$9{\cdot}20\times10^{-3}$	108·7
4	1154·6	22·1	1	10^{-3}	$1{\cdot}088\times10^{-2}$	$5{\cdot}515\times10^{5}$	$5{\cdot}54\times10^{-2}$	18·04
5	1235·2	90·1	2	10^{-4}	$2{\cdot}923\times10^{-3}$	$1{\cdot}642\times10^{7}$	$2{\cdot}63\times10^{-2}$	38·08
6	1345·9	14·7	4·5	4×10^{-4}	$5{\cdot}619\times10^{-2}$	$2{\cdot}059\times10^{6}$	$3{\cdot}36\times10^{-1}$	2·979
7	1390·2	4·66	6	10^{-3}	$2{\cdot}936\times10^{-1}$	$5{\cdot}147\times10^{5}$	1·36	0·7331

TABLE 1. Physical conditions and parameters for the examples of bubble growth in superheated sodium given in the present study.

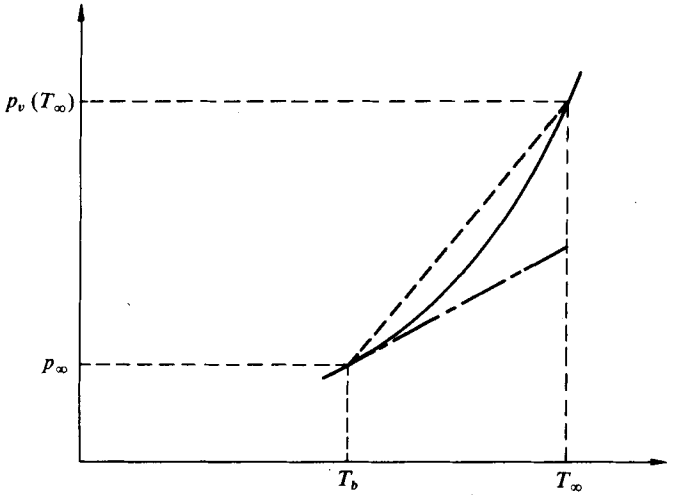

FIGURE 4. The solid curve indicates the correct vapour-pressure dependence on temperature. The dashed line is the 'chord approximation' of (20). The dash–dot line is the 'tangent approximation' to the vapour pressure used by Mikic *et al.* (1970).

We remark that by definition $p_\infty = p_v(T_b)$. It is evident that (20) makes it possible to combine (5) and (19) explicitly. We now introduce a dimensionless time variable

$$\tau = \frac{\alpha}{R_0^4}\int_0^t R^4(t')\,dt', \tag{21}$$

where

$$\alpha = [p_v(T_\infty) - p_\infty]^{\frac{3}{2}}/2\sigma(T_\infty)\rho^{\frac{1}{2}}. \tag{22}$$

We also use the normalized bubble volume

$$V = (R/R_0)^3 \tag{23}$$

in place of the radius. With these substitutions we obtain the dynamical equation

$$V^{\frac{4}{3}}\left[V\frac{d^2V}{d\tau^2} + \frac{7}{6}\left(\frac{dV}{d\tau}\right)^2\right] = 3\left[1 - \mu\int_0^\tau (\tau-\theta)^{-\frac{1}{2}}\frac{dV}{d\theta}\,d\theta - V^{-\frac{1}{3}}\right], \tag{24}$$

with the initial condition $V(0) = 1$ and with the parameter μ given by

$$\mu = \frac{1}{3}\left(\frac{2\sigma D}{\pi}\right)^{\frac{1}{2}} \rho_v \frac{L}{k}(T_\infty - T_b)^{-1}\{\rho[p_v(T_\infty) - p_\infty]\}^{-\frac{1}{2}}. \tag{25}$$

All the physical parameters of the problem are contained in μ, and should all be evaluated at the temperature T_b except σ, which is evaluated at T_∞.

In (24) the left-hand side represents the effect of the liquid inertia while on the right-hand side the last term gives the effect of surface tension and the second term, which is proportional to μ, describes the decrease in the internal pressure caused by the thermal effect. As long as the growth continues, this term increases monotonically from zero, and its effect on the bubble growth process appears sooner the larger the value of the parameter μ. This parameter decreases with increasing superheat or with decreasing ambient pressure. This behaviour is shown in figure 5 for liquid sodium and water. Similar curves for α are shown in figure 6.

Equation (24) has been obtained through the introduction of several simplifying assumptions some of which, like (20), may appear rather drastic. It is therefore of interest to compare the results obtained from its integration with the ones described earlier derived from (5) and (19). This comparison is shown in figure 1 for the growth velocity, in figure 2 for the surface temperature and in figure 3 for the radius. The results from (24) are indicated by broken lines in these figures except for the cases in which they are indistinguishable from those discussed above. The values of the relevant parameters μ, α, R_0 and ΔT are given in table 1. The high superheat cases ($p_\infty = 0{\cdot}5$ atm, $\Delta T = 340$ °K; $p_\infty = 1$ atm, $\Delta T = 279$ °K and $\Delta T = 133$ °K) all show serious discrepancies in the growth rates and in the surface temperature behaviour. However, it will be observed that the differences in the radii are much smaller, at least in the range of values ($R \lesssim 0{\cdot}5$–1 cm) of practical interest. It should be remarked that for larger radii many assumptions of the mathematical model become questionable, such as the assumption of spherical symmetry and the neglect of relative translational motion between the bubble and the liquid. The case of 90 °K superheat is a particularly interesting test of the validity of the approximate equation (24). Here the superheat is only moderately large, so that, unlike the high superheat cases, thermal effects become significant while the radius is still in the range of practical interest. It is observed that, although some discrepancy exists in the growth rate (figure 1*b*) and in the surface temperature behaviour (figure 2*a*), these differences have a negligible effect on the radius. Finally, the low superheat cases all show an excellent agreement between the results obtained from (24) and those illustrated earlier. In summary, we may say that, although (24) is not a good approximation to the theory based on (5) and (19) for very large superheats, the differences between the two approaches become significant in practice only for values of the radius which appear to be of little practical interest. Although our results justify this statement only for liquid sodium, we believe that its validity is entirely general except perhaps for temperatures and pressures near the critical point. The basis for this view is that for very high superheats inertial effects dominate most of the portion of bubble growth of practical significance, and it is clear from the preceding considerations that these inertial effects are correctly accounted for in the present formulation.

We should also like to comment on the fact that the dashed curves in figures 1(*a*) and (*b*) lie consistently above those obtained from the more accurate theory, a

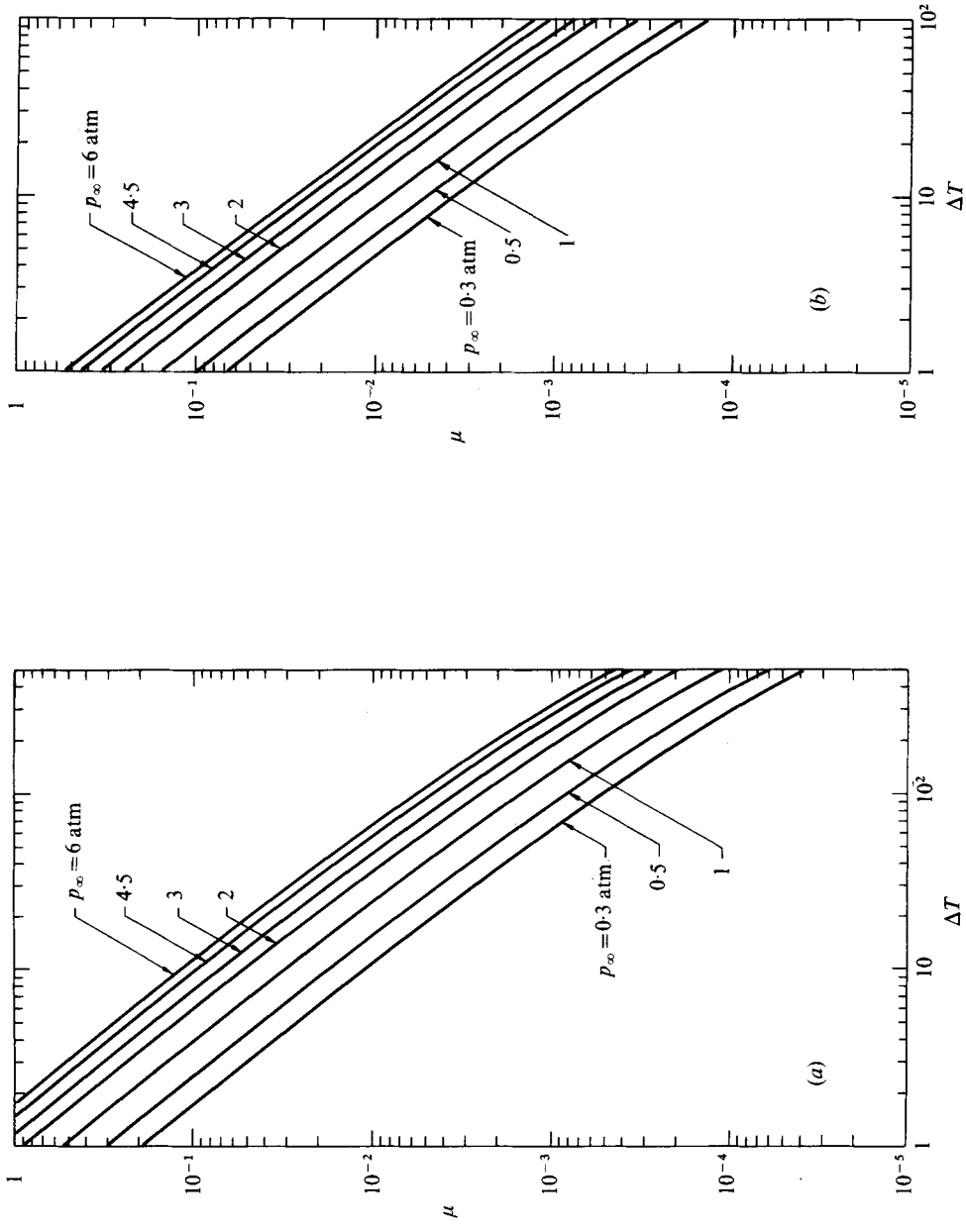

FIGURE 5. The dependence of the parameter μ given in (25) on superheat for various ambient pressures p_∞ for (*a*) sodium and (*b*) water.

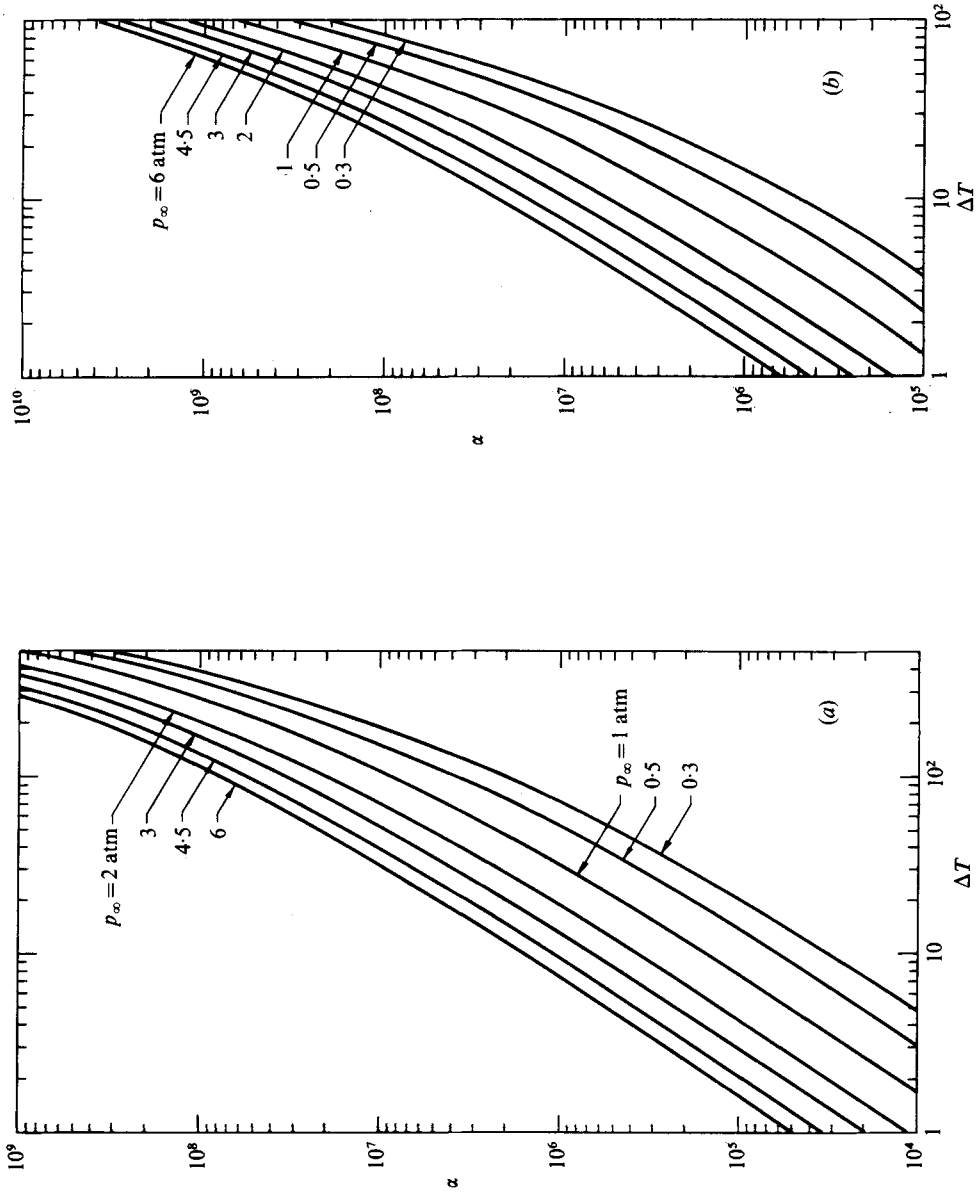

FIGURE 6. The dependence of the parameter α given in (22) on superheat for various ambient pressures p_∞ for (*a*) sodium and (*b*) water.

behaviour which shows higher growth rates. This feature is consistent with the approximations introduced in order to derive (24) since the evaluation of ρ_v at T_b rather than at the instantaneous value of T_s diminishes the latent-heat requirement. In addition, as figure 4 shows, the linear law of pressure variation, equation (20), tends to overestimate the bubble internal pressure for a fixed value of T_s.

The limiting behaviour of $R(t)$ discussed above in § 2 is readily obtainable from (24). For the initial stages of the growth, in which the integral on the right-hand side can be neglected, one integration can readily be performed with the result

$$\left(\frac{dV}{d\tau}\right)^2 = V^{-\frac{7}{3}}\left(\frac{dV}{d\tau}\right)_0^2 + 6V^{-\frac{4}{3}}(1-\tfrac{3}{2}V^{-\frac{1}{3}}), \tag{26}$$

where $(dV/d\tau)_0$ is the initial velocity. If the value of μ is so small that (26) still applies when $V \gg 1$, we have to leading order

$$dV/d\tau \simeq 6^{\frac{1}{2}}V^{-\frac{2}{3}}, \tag{27}$$

which is readily seen to be exactly equivalent to (2). For late times, inertial and surface-tension effects become negligible and (24) reduces to

$$\mu\int_0^\tau (\tau-\theta)^{-\frac{1}{2}}\frac{dV}{d\theta}d\theta \simeq 1,$$

which can readily be inverted to give

$$dV/d\tau \simeq 1/\pi\mu\tau^{\frac{1}{2}}, \tag{28}$$

which, by use of (21), can be seen to coincide with (3).

5. The scaled growth formulation

Let us now make the following change of variables in (24):

$$y = \mu^6 V, \quad x = \mu^{10}\tau. \tag{29}$$

This equation then becomes

$$y^{\frac{4}{3}}\left[y\frac{d^2y}{dx^2}+\frac{7}{6}\left(\frac{dy}{dx}\right)^2\right] = 3\left[1-\int_0^x (x-\xi)^{-\frac{1}{2}}\frac{dy}{d\xi}d\xi - \mu^2 y^{-\frac{1}{3}}\right], \tag{30}$$

with the initial condition

$$y(0) = \mu^6. \tag{31}$$

The asymptotic behaviours (27) and (28) are readily seen to be independent of μ. It is clear, therefore, that the effect of the parameter μ on the solution of (30) becomes negligible as soon as $\mu^2 y^{-\frac{1}{3}} \ll 1$, which, as will be seen below, means in practice an order-of-magnitude increase in the bubble radius. The scaling (29) can be referred to the physical variables R and t with the definitions

$$\tilde{R} = \mu^2 R/R_0, \quad \tilde{t} = \alpha\mu^2 t. \tag{32}$$

From (21) and (23) it is readily seen that these equations imply

$$\tilde{R} = y^{\frac{1}{3}}, \quad \tilde{t} = \int_0^x y^{-\frac{4}{3}}(\xi)\,d\xi, \tag{33}$$

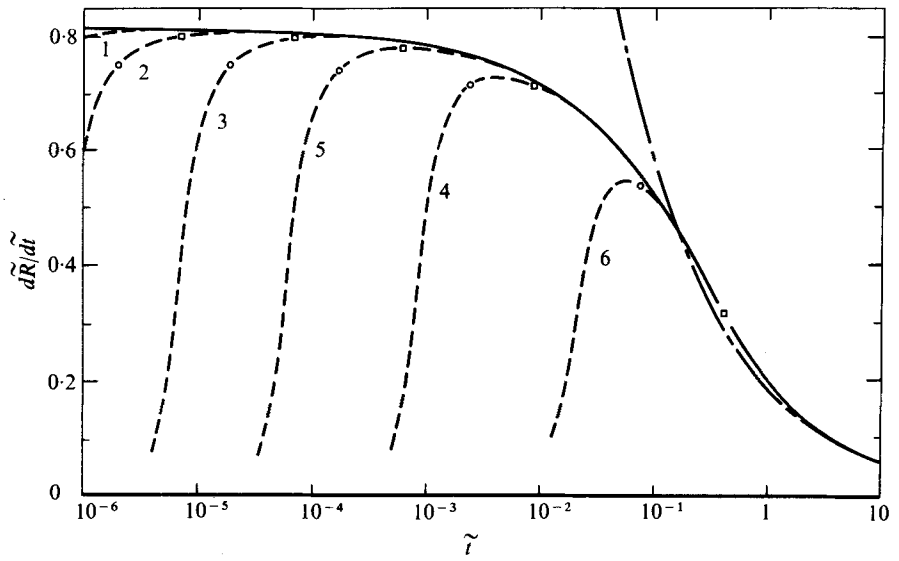

FIGURE 7. The scaled growth rate given by (34) is shown as a function of the dimensionless time (32) by the solid line. The non-scaled, μ-dependent portion of the growth as determined by (30) is shown by dashed lines which merge into the general scaled curve. The open circles on the dashed lines give the times at which $R = 10R_0$; the open squares give the times at which $R = 50R_0$. The numbers refer to the conditions given in table 1. The dash–dot line is the purely thermally controlled growth (35); i.e. $\pi^{-1}(3\tilde{t})^{-\frac{1}{2}}$.

and therefore that the relation

$$\tilde{R} = \tilde{R}(\tilde{t}) \tag{34}$$

is independent of the physical parameters α and μ except in the initial (and usually unimportant) stages of the growth. In terms of the scaled variables $\tilde{R}$ and $\tilde{t}$ the asymptotic relations (2) and (3) are

$$\left(\frac{d\tilde{R}}{d\tilde{t}}\right)_{\text{inertial}} = (\tfrac{2}{3})^{\frac{1}{2}}, \quad \left(\frac{d\tilde{R}}{d\tilde{t}}\right)_{\text{thermal}} = \pi^{-1}(3\tilde{t})^{-\frac{1}{2}}. \tag{35}$$

Figure 7 shows a graph of the scaled radial growth velocity $d\tilde{R}/d\tilde{t}$ as determined by (30) as a function of the scaled time $\tilde{t}$. The initial, non-scaled stages of the growth are also indicated for a range of values of μ. The open circles on the curves give the points at which $R = 10R_0$ and the squares the points at which $R = 50R_0$. The confluence of all the solutions into a single curve is a graphic demonstration of the validity of (34). In the figure the thermally controlled growth velocity (35) is also shown. The limited applicability of this often-used relation is apparent.

In view of the approximations which lead from (5) and (19) to (24) or (30), it is of course of interest to show the results obtained from the complete theory in terms of the scaled variables (32) and to compare them with (34). Such a comparison is provided in figure 8 for the growth rates and in figure 9 for the radius *vs.* time behaviour. Apart from the initial stages of the growth, the differences already illustrated in figures 1 and 3 are of course still present here. In particular the scaled growth rates for very large superheat are seen to deviate considerably from those given by (34). However, figure 9 shows that these discrepancies have limited effects on the $R(t)$ results. It may

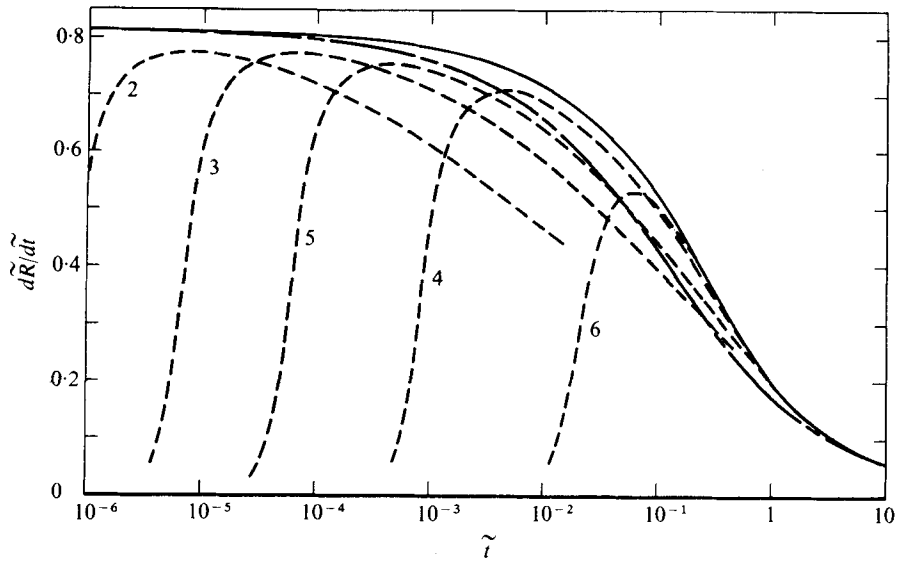

FIGURE 8. The scaled growth rate given by (34) (the solid line) is compared with the accurate growth rates given by (5) and (19) (the dashed lines). These accurate growth rates are those given in figure 1. The numbers refer to the conditions given in table 1. The dash–dot line shows the growth rate determined from (39).

therefore be concluded that the parameters α and μ do include in a physically meaningful way all the quantities relevant for the growth of vapour bubbles in superheated liquids under a very wide range of conditions. Likewise, the scaling (32) and the relation (34) embody correctly, although in an approximate way, the characteristics of the physical process under consideration. In the cases of high superheat it may be possible to evaluate the physical properties appearing in the parameters μ and α at a temperature different from T_b in order to give a better agreement with the more complete theory based on (5) and (19). However, it would be difficult to give a simple prescription of general applicability, and therefore we have not explored this possibility.

If L and ρ_v are taken to be independent of temperature, it is also possible to write the equation for the temperature, equation (19), in terms of scaled variables. It is easy to show that

$$T_\infty - T_s = (T_\infty - T_b) \int_0^x (x-\xi)^{-\frac{1}{2}} \frac{dy}{d\xi} d\xi.$$

If we now define a dimensionless temperature as

$$\tilde{T}_s = (T_s - T_b)/(T_\infty - T_b),$$

we obtain from (33)

$$\tilde{T}_s = \tilde{T}_s(\tilde{t}).$$

A graph of this relation is given in figure 10, where it is compared with the results obtained from (5) and (19).

It is of interest to compare our results with a simple interpolation expression for bubble growth proposed by Mikic *et al.* (1970). This expression is also written in terms of scaled variables R^+ and t^+ and is given by

$$R^+ = \tfrac{2}{3}[(t^+ + 1)^{\frac{3}{2}} - (t^+)^{\frac{3}{2}} - 1], \tag{36}$$

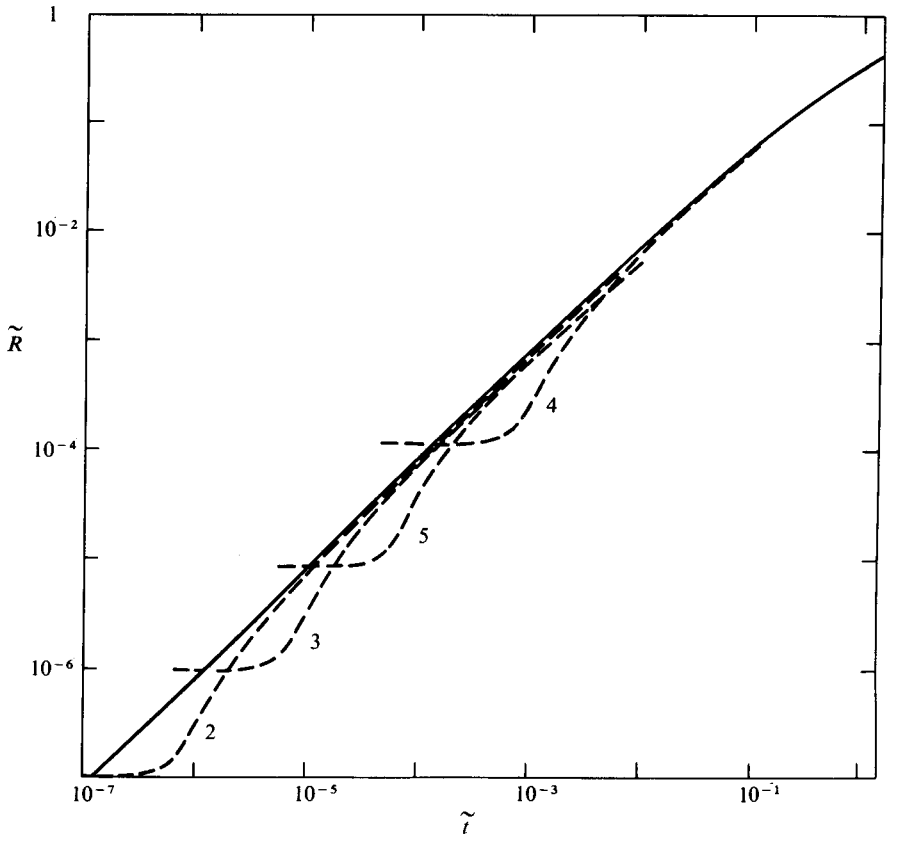

FIGURE 9. The scaled radius given by (34) is shown as a function of time by the solid line. The bubble radius and the time are made dimensionless according to (32). The dashed lines give the accurate radii determined from (5) and (19); these accurate radii are also shown in figure 3. The numbers refer to the conditions given in table 1.

where
$$R^+ = (A/B^2)R, \quad t^+ = (A^2/B^2)t \tag{37}$$

and
$$A = \left(\frac{2}{3}\frac{T_\infty - T_b}{\rho}\frac{dp_v}{dt}\right)^{\frac{1}{2}}, \quad B = \left(\frac{12}{\pi D}\right)^{\frac{1}{2}}\frac{k}{L\rho_v}(T_0 - T_b). \tag{38}$$

In their paper Mikic *et al.* (1970) used the Clausius–Clapeyron relation to evaluate dp_v/dT at the boiling temperature T_b. With this choice the inertia-controlled portion of the growth cannot be described correctly for moderate or large superheats. A substantial improvement was suggested by Theofanous & Patel (1976), who used an approximate linear law [our equation (20)] for the evaluation of the derivative, setting $dp_v/dT \simeq [p_\infty(T_\infty) - p_\infty]/(T_\infty - T_b)$. Following this procedure and evaluating the physical properties appearing in (38) at the boiling temperature, one can readily show that the scaling (37) is identical with our equation (32).† In terms of the variables defined by (32), equation (36) becomes

$$\tilde{R} = (2/\pi^2)\,(\tfrac{2}{3})^{\frac{1}{2}}\,[(\tfrac{1}{2}\pi^2\tilde{t}+1)^{\frac{3}{2}} - (\tfrac{1}{2}\pi^2\tilde{t})^{\frac{3}{2}} - 1]. \tag{39}$$

† Notice that the quantities μ^2/R_0 and $\alpha\mu^2$ appearing in (32) are independent of surface tension provided that this quantity is consistently evaluated at the initial temperature T_∞.

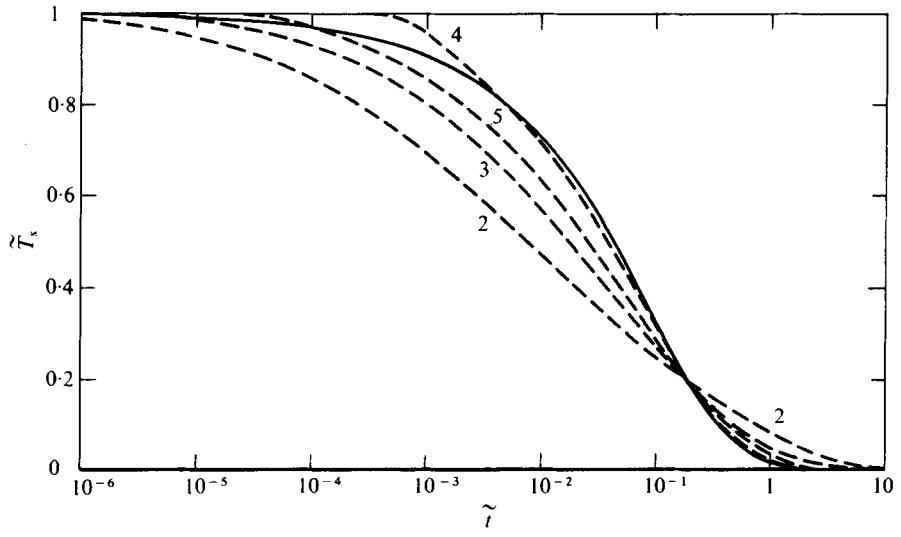

FIGURE 10. The scaled temperature at the bubble boundary is shown as a function of the dimensionless time by the solid line. The accurate temperatures determined from (5) and (19) are shown by the dashed lines. These accurate temperatures are also shown in figure 2. The numbers refer to the conditions given in table 1.

The growth rate predicted by this equation is also illustrated in figure 8, which shows (36) or (39) to be an acceptable interpolation between the inertia-controlled and the asymptotic stages. The radius–time behaviour given by (39) follows quite closely the full line on figure 9, and is not shown for clarity. In view of the rather unsatisfactory physical basis on which (36) and (39) have been obtained, the close agreement with the more precise theory is rather surprising. Nevertheless, the possibility of describing vapour-bubble growth by means of this interpolation, even though approximate, is useful.

Both (34) and (39) apply only for bubbles that have grown at least an order of magnitude from their initial size. It may therefore be of value to be able to estimate the time from which they begin to be valid. To this end we show in figure 11 a graph of the time needed to attain the sizes $10R_0$, $20R_0$, $50R_0$ and $100R_0$ as a function of the parameter μ. The initial conditions for the continuous lines are $R(0) = R_0$ and $dR(0)/dt = 0{\cdot}04\alpha R_0$. The broken line and the dash–dot line have been obtained from the same $R(0)$, but with initial velocities an order of magnitude greater and smaller than the value just given. The small influence of the initial condition is clear from this figure.

As a final point we should like to show that it is possible to define a more general scaling for bubble growth which is capable of accounting also for the surface-tension-dominated latency stage. This more general scaling, however, is less useful than the one considered above.

It is easy to show that, if the difference $p_v(T_s) - p_\infty$ is kept constant in (5), as is approximately correct during the latency stage, one can obtain a first integral analogous to (26), namely

$$\left(\frac{dR}{dt}\right)^2 = \left(\frac{dR}{dt}\right)_0^2 \left(\frac{R_0}{R}\right)^3 + \frac{2}{3}\frac{p_v(T_\infty) - p_\infty}{\rho}\left[1 - \left(\frac{R_0}{R}\right)^3\right]\left[1 - \frac{3}{2}\frac{R_0}{R}\frac{1-(R_0/R)^2}{1-(R_0/R)^3}\right]. \quad (40)$$

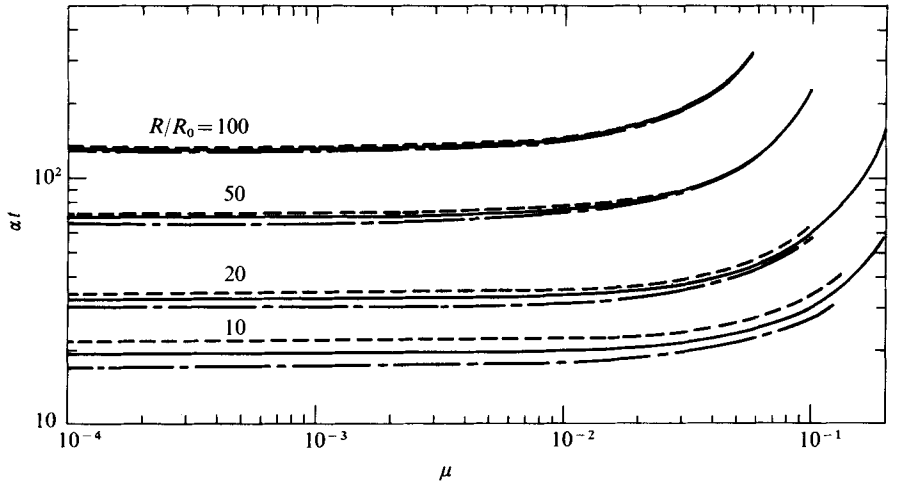

FIGURE 11. The times required for growth to the values of R/R_0 indicated are shown as a function of μ. The time is scaled according to (41). The solid lines correspond to the initial conditions $R = R_0$ and $dR/dt = 0{\cdot}04\alpha R_0$. The dashed lines and the dash–dot lines correspond to initial conditions $R = R_0$ and $dR/dt = 0{\cdot}004\alpha R_0$ and $dR/dt = 0{\cdot}40\alpha R_0$, respectively.

Here $(dR/dt)_0$ is the initial velocity which upsets the unstable equilibrium at the initial radius, and (1) has been used to eliminate the surface-tension parameter.† Now it is obvious that, for fixed $(dR/dt)_0/(\alpha R_0)$, (40) admits the scaling

$$R_* = R/R_0, \quad t_* = \alpha t, \tag{41}$$

with α defined by (22). We note that, although the scaling (41) is different from (32), one has $R_*/t_* = \tilde{R}/\tilde{t}$, so that a relation of the type

$$d\tilde{R}/d\tilde{t} = f(\tilde{R}/\tilde{t}) \tag{42}$$

describes the bubble behaviour both in the latency stage (in which $T_s \sim T_\infty$) and in the successive stages of growth. Although in principle (42) contains all the information needed for the description of the process, it is clear that a graphical presentation of it would be of limited practical value.

This study is a portion of a programme supported by the National Science Foundation under Grant ENG 75-22676. One of us (AP) wishes to thank the Gruppo Nazionale per la Fisica Matematica del Consiglio Nazionale delle Ricerche for partial support during this study.

REFERENCES

BANKOFF, S. G. 1964 Asymptotic growth of a bubble in a liquid with uniform initial superheat. *Appl. Sci. Res.* A **12**, 267–281.

BIRKHOFF, G., MARGULIES, R. S. & HORNING, W. A. 1958 Spherical bubble growth. *Phys. Fluids* **1**, 201–204.

DALLE DONNE, M. & FERRANTI, M. P. 1975 The growth of vapor bubbles in superheated sodium. *Int. J. Heat Mass Transfer* **18**, 477–493.

† Notice that (2) can be obtained directly from (40) in the limit $R_0/R \to 0$.

HSIEH, D. Y. 1965 Some analytical aspects of bubble dynamics. *J. Basic Engng, A.S.M.E.* D **87**, 991–1005.

MIKIC, B. B., ROHSENOW, W. M. & GRIFFITH, P. 1970 On bubble growth rates. *Int. J. Heat Mass Transfer* **13**, 657–666.

PLESSET, M. S. & PROSPERETTI, A. 1977 Bubble dynamics and cavitation. *Ann. Rev. Fluid Mech.* **9**, 145–185.

PLESSET, M. S. & ZWICK, S. A. 1952 A nonsteady heat diffusion problem with spherical symmetry. *J. Appl. Phys.* **23**, 95–98.

PLESSET, M. S. & ZWICK, S. A. 1954 The growth of vapor bubbles in superheated liquids. *J. Appl. Phys.* **25**, 493–500.

PLESSET, M. S. & ZWICK, S. A. 1955 On the dynamics of small vapor bubbles in liquids. *J. Math. Phys.* **33**, 308–330.

ROHSENOW, W. M. 1971 Boiling. *Ann. Rev. Fluid Mech.* **3**, 211–236.

SCRIVEN, L. E. 1959 On the dynamics of phase growth. *Chem. Engng Sci.* **10**, 1–13.

THEOFANOUS, T., BIASI, L., ISBIN, H. S. & FAUSKE, H. 1969 A theoretical study of bubble growth in constant and time-dependent pressure fields. *Chem. Engng Sci.* **24**, 885–897.

THEOFANOUS, T. G. & PATEL, P. D. 1976 Universal relations for bubble growth. *Int. J. Heat Mass Transfer* **19**, 425–429.

ZUBER, N. 1961 The dynamics of vapor bubbles in non-uniform temperature fields. *Int. J. Heat Mass Transfer* **2**, 83–98.

ZWICK, S. A. 1960 The growth of vapor bubbles in a rapidly heated liquid. *Phys. Fluids* **3**, 685–692.